Unicycle With Only Range Input: An Array of Patterns

Twinkle Tripathy, *Student Member, IEEE*, and Arpita Sinha, *Member, IEEE*

***Abstract*—The objective of this paper is to generate planar patterns using an autonomous agent modeled as a unicycle. The patterns are generated about a stationary point referred to as the target. To achieve the same, the paper proposes a family of control inputs that are continuous functions of range, which is the distance between the unicycle and the target. The paper studies in detail a characterization of the resulting trajectories, which are a plethora of patterns of parametric curves (circles, spirals, epicyclic curves like hypotrochoids) and more. These appealing patterns find applications in exploration, coverage, land mine detection, etc., where the target represents any point of interest like a landmark or a beacon. The paper also investigates the necessary conditions on the control laws in order to generate patterns of desired shapes and bounds. Furthermore, to generate desired patterns with arbitrary initial conditions, a switching strategy is proposed which is illustrated using an algorithm. The paper presents a series of simulations of appealing patterns generated using the proposed control laws.**

***Index Terms*—Non-holonomic kinematics, path planning, pattern generation, range information, unicycle.**

I. Introduction

NATURE is filled with a myriad of patterns. These patterns are rich in diversity ranging from microscopic to macroscopic levels. To list a few, patterns can be seen in bacterial colonies, fractals in flora and fauna, stripes and spots in animals, vegetation patterns, shapes of galaxies and planetary motions with respect to the sun and the moon. Apart from their aesthetic beauty, these patterns serve applications like demining, area monitoring, exploration, coverage [1], [2].

These innumerable naturally occurring patterns have drawn the interest of the research community on robotics and control over the past decades. The literature in the area of pattern generation is replete with a wide variety of mathematical patterns, starting from simple lines, triangles, circles to complex spirals, hypotrochoids, etc. These patterns are generated by using either single or multiple autonomous agents with different kinds of kinematic models like linear, unicycle, and double integrator. For multi-agent systems, patterns can be generated through inter-agent spatial arrangements. This problem is referred to as formation control wherein the inter-agent global formations render a variety of patterns. The developments in the area of formation control problem have been surveyed by Oh *et al.* [3]. The global formation patterns of multiple agents could be stationary or dynamic in space. For example, there exist results for simple stationary formations where the agents arrange themselves in two-dimensional (2-D) lines, circles, and polygons [4], [5]. Dynamic (translationally and/or rotationally invariant with time) formations have also been explored in the literature [6]–[9]. Formations have been achieved in 3-D spaces as well [10].

The generation of patterns has also been explored by controlling the trajectories of the agents while they maintain a spatial formation [11]–[16]. It is also possible to trace patterns by guiding autonomous agents to follow any prespecified trajectories whether independently (single-agent) or cooperatively (multiagent) [17]–[19].

The proposed framework of the paper is in close relation with the work presented in [11]–[16]. In [11], Galloway *et al.* examine the nonlinear closed-loop dynamics of the constant bearing based cyclic pursuit strategy for unit masses tracing out twice differentiable curves in a plane and reveal the existence of periodic orbits. The authors extend their analysis in [12] to investigate low-dimensional cases of cyclic pursuit where each agent employs a constant bearing steering law relative to only one agent. By using bifurcation for a set of collinear equilibria, they show the existence of periodic trajectories of the agents. In [13], Marshall *et al.* achieve stable periodic formations by employing cyclic pursuit strategy for multiple agents modeled as unicycles. The authors present an analysis to conjecture the existence of periodic trajectories of the agents while they maintain a dynamic formation with respect to each other. By introducing an additional rotation and stabilization term in [14], Juang proposes a generalization of the cyclic pursuit control scheme. The work uses agents with single integrator kinematics. The distribution of the roots governs the resulting formation arising out of the agents' trajectories based on the count of the imaginary axis eigenvalues. Intricate epicyclic patterns result with appropriate conditions on the control law parameters and initial conditions. In [15] and [16], with an extension to the standard feedback for the multiagent consensus problems, Tsiotras *et al.* achieve global formations with multiple agents modeled with single integrator kinematics. The authors augment the control law with a term represented as a product of an error term with a

Manuscript received August 23, 2016; revised April 16, 2017 and July 18, 2017; accepted July 27, 2017. Date of publication August 7, 2017; date of current version April 24, 2018. Recommended by Associate Editor S. Andersson. *(Corresponding author: Twinkle Tripathy.)*

The authors are with the Systems and Control Engineering, Indian Institute of Technology Bombay, Mumbai 400076, India (e-mail: twinkle.tripathy@sc.iitb.ac.in; arpita.sinha@iitb.ac.in).

Color versions of one or more of the figures in this paper are available online at http://ieeexplore.ieee.org.

Digital Object Identifier 10.1109/TAC.2017.2736940

skew symmetric matrix. This improves the flexibility of the law not only with respect to the possible rendezvous points, but also with patterns.

In contrast to the work presented in [11]–[16], this paper focuses on generating parametric curves and many more patterns in a plane with a single autonomous agent, modeled as a unicycle. The patterns are formed about a point which we refer to as the target. The target point is pre-specified and can be representative of any landmark, building of interest, etc. The control input is based on range measurement only, where range is the distance between the agent and target. A preliminary analysis, with the input as a linear function of range, is presented in [20]–[22], which gives hypotrochoid-like patterns. In [23], we present an analysis for a monomial function of range as input. This results in the generation of a wider set of hypotrochoid-like patterns.

This work proposes the control input to be any continuous function of range. This offers the advantage of the generation of a wide spectrum of patterns namely circles, hypotrochoid-like patterns, epitrochoid-like patterns, spirals, and many more mathematical curves, by the use of only range information. For the given framework, we highlight the major contributions of the paper:

1) *Characterizing the trajectory:* Under the proposed control input, the trajectory of the unicycle is either a bounded (annular as shown in Fig. 1(a) or circular) or an unbounded pattern [as shown in Fig. 1(b)].
2) *Conditions for desired patterns:* In order to generate a desired pattern, we propose the conditions that the control input needs to satisfy. We also propose ways to find the initial conditions and the range of values the initial conditions can take.
3) *Designing a switching control law:* In case the given initial conditions are not satisfactory for a desired pattern, we propose a switching control strategy. This strategy ensures that the desired pattern is generated starting from any initial condition.

The paper is organized in the following manner: Section II defines the problem statement for the generation of planar patterns in the given framework. Section III introduces the terminologies used throughout the paper and discusses the preliminaries necessary for further analysis. Section IV gives a characterization of the unicycle trajectories for any continuous function of range as the control input. The generation of desired patterns with arbitrary initial conditions is explored in Section V. Section VI discusses the design of certain types of patterns and shows a variety of other patterns that can be generated in the given framework. Finally, Section VII concludes the paper with a glimpse into the possible future directions.

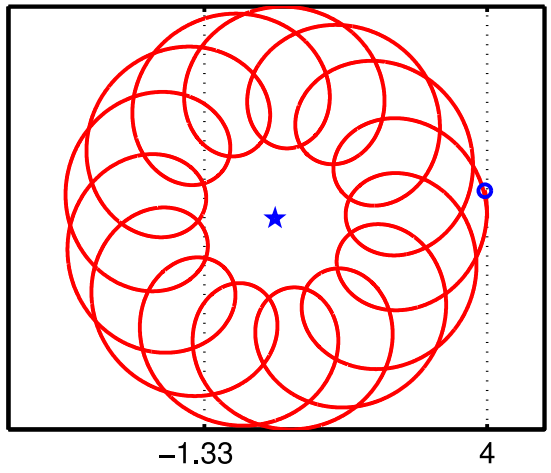

Fig. 1. Trajectories of the unicycle. (a) Annular pattern. (b) Unbounded pattern.

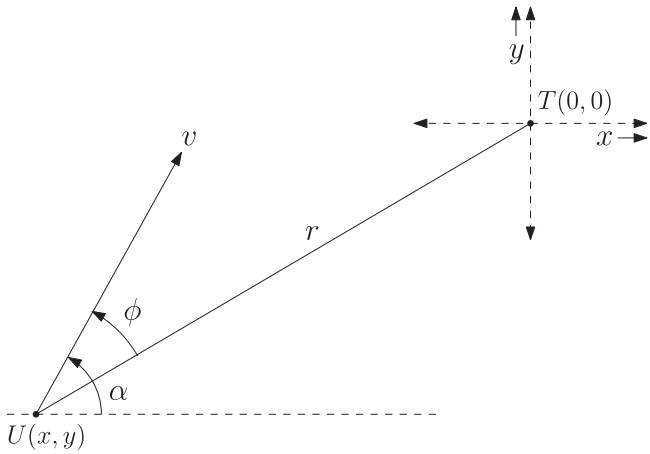

Fig. 2. Planar geometry between the robot and the target point.

II. Problem Description

The paper addresses the problem of characterizing the trajectories of a unicycle to render a plethora of beautiful patterns in a plane. We only use the range information to generate the patterns, where range (denoted by r) is the line-of-sight distance between the unicycle and a stationary point denoted as the target T. Without loss of generality, the target is assumed to be at origin. The planar geometry between target and agent is depicted in Fig. 2. In this paper, we use $\mathbb{R}$ as the set of real numbers and C^1 as the set of continuously differentiable functions.

The kinematics of the unicycle are given by

$$\dot{x}(t) = v\ \cos\alpha(t),\ \dot{y}(t) = v\sin\alpha(t),\ \dot{\alpha}(t) = u(t) \quad (1)$$

where $(x(t), y(t))$ is the position coordinate of the unicycle at time t, v is the constant linear speed, $\alpha(t)$ is the heading direction, and $u(t)$ is the control input. As a function of range, the input is designed as

$$u = f(r) \quad (2)$$

such that $f(r) : \mathbb{R} \mapsto \mathbb{R}$ is continuous. The analysis can be extended to functions that are locally Lipschitz. We denote ϕ as the angle between the line of sight and the heading. With reference to Fig. 2, we transform (1) into polar coordinates, combine it with (2) and then incorporate the variable ϕ to get

$$\dot{r} = -v\cos\phi, \quad r\dot{\phi} = rf(r) + v\sin\phi. \quad (3)$$

Computing $dr/d\phi$ and then rearranging gives $(rf(r) + v\sin\phi)dr + vr\cos\phi\, d\phi = 0$. The differential equation may or may not be exact. When the equation is not exact, an integrating factor is used to make it exact [24]. Nevertheless, the solution of the differential equation always takes the form

$$\tilde{f}(r) + vr\sin\phi = K \quad (4)$$

where $K \in \mathbb{R}$ is the constant of integration and $\tilde{f}(r) \in C^1$ is devoid of any constant term and satisfies $f(r) = \frac{1}{r}\frac{d}{dr}\tilde{f}(r)$. When the initial conditions $r_0 (= r(0))$ and $\phi_0 (= \phi(0))$ along with the control input $f(r)$ are specified, then

$$K = \tilde{f}(r_0) + vr_0\sin\phi_0. \quad (5)$$

For different values of K, (4) produces a family of level curves. For any K, every point (r, ϕ) on the level curve is a solution of (3). Now, if K is specified, we are interested to find the feasible set of initial conditions and the instantaneous $(r(t), \phi(t))$ for all $t \geq 0$ and $K \in \mathbb{R}$ under the control input $f(r)$. We begin by rearranging (4) as

$$g_K(r) = -vr\sin\phi \quad (6)$$

where $g_K(r) = \tilde{f}(r) - K$. Then

$$f(r) = \frac{1}{r}\frac{d}{dr}g_K(r). \quad (7)$$

Obviously, $g_K(r) \in C^1$. Given $f(r)$ and K, (6) holds only when $-vr \leq g_K(r) \leq vr$, as otherwise $\sin\phi$ becomes undefined. Whenever $-vr \leq g_K(r) \leq vr$ for a given r, the corresponding $\phi = \{\sin^{-1}(-\frac{g_K(r)}{vr}), \pi - \sin^{-1}(-\frac{g_K(r)}{vr})\}$. Next, we introduce the terminologies used in the paper. We also discuss the properties of $g_K(r)$ using the proposed terminologies that play a crucial role in further analysis.

III. Preliminaries

This section presents the set of terminologies used throughout the paper and lays down the necessary preliminaries before we proceed with further analysis.

To begin with, we define

$$\mathcal{S}_K(f) := \{r \geq 0 \mid -vr \leq g_K(r) \leq vr\} \quad (8)$$

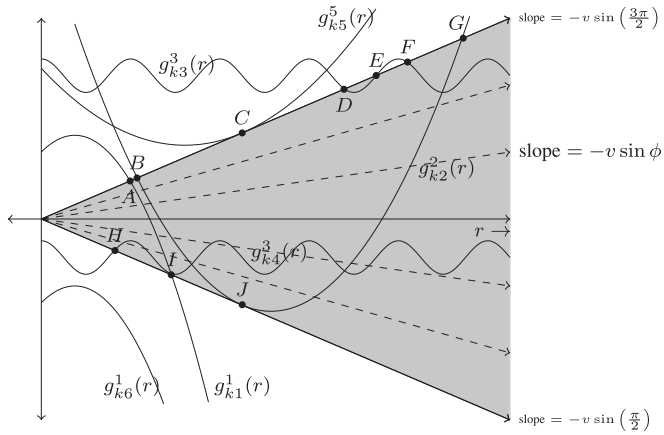

Fig. 3. Types of intervals of $\mathcal{S}_K(f)$.

as the set of feasible values of r that satisfy (6) for given $f(r)$ and K.

Fig. 3 shows plots of different $g_K(r)$ functions where $g^i_K(r)$ denotes the ith $g_K(r)$ function. The straight lines represent $vr\sin\phi$ for different values of ϕ. The region between the straight lines $\pm vr$ (corresponding to $\sin\phi = \pm 1$), shaded in gray, denotes the values of (r, ϕ) that could satisfy (6). Thus, the shaded region denotes a feasible region in which we study the behavior of $g_K(r)$. In Fig. 3, let r_i, $i = A, B, \ldots, J$ be the values of r at the points $A, B, \ldots, J$. The set $\mathcal{S}_K(f)$ is a set of intervals in $\mathbb{R}$. For example, $\mathcal{S}_K(f) = [r_A, r_I]$ for $g^1_{k1}(r)$ in Fig. 3. To characterize different types of intervals in $\mathcal{S}_K(f)$, we introduce the following sets:

1) *Entry points:* $\bar{r}$ is an entry point if there exists $\delta_1 > 0$ such that $[\bar{r}, \bar{r} + \delta_1) \in \mathcal{S}_K(f)$ and, for all $\delta_2 > 0$, $(\bar{r} - \delta_2, \bar{r}) \notin \mathcal{S}_K(f)$. We define the set of all such points as

$$E_n(g_K) = \{r \geq 0 \mid \text{either } g_K(r) = vr \text{ and } dg_K(r)/dr < v \text{ or } g_K(r) = -vr \text{ and } dg_K(r)/dr > -v\}. \quad (9)$$

Graphically, at an entry point, $g_K(r)$ enters the shaded region in Fig. 3.

2) *Tangential points:* $\bar{r}$ is a tangential point if $g_K(r)$ is tangent to either of the straight lines $\pm vr$ at $\bar{r}$. Let us denote this set by

$$E_t(g_K) = \{r \geq 0 \mid \text{either } g_K(r) = vr \text{ and } dg_K(r)/dr = v \text{ or } g_K(r) = -vr \text{ and } dg_K(r)/dr = -v\}. \quad (10)$$

3) *Exit points:* At an exit point $\bar{r}$, for all $\delta_1 > 0$, $(\bar{r}, \bar{r} + \delta_1) \notin \mathcal{S}_K(f)$ and there exists $\delta_2 > 0$ such that $(\bar{r} - \delta_2, \bar{r}] \in \mathcal{S}_K(f)$. We define the set of all such points as

$$E_x(g_K) = \{r \geq 0 \mid \text{either } g_K(r) = vr \text{ and } dg_K(r)/dr > v \text{ or } g_K(r) = -vr \text{ and } dg_K(r)/dr < -v\}. \quad (11)$$

An exit point marks a point where any $g_K(r)$ exits the shaded region in Fig. 3.

Example: In Fig. 3, $r_A \in E_n(g^1_{k1})$, $r_B \in E_n(g^2_{k2})$, $\{r_D, r_F\} \in E_n(g^3_{k3})$, and $r_H \in E_n(g^3_{k4})$ are entry points. $r_C \in E_t(g^5_{k5})$, $r_I \in E_t(g^3_{k4})$, and $r_J \in E_t(g^2_{k2})$ are tangential points. Fig. 3 shows exit points as $r_E \in E_x(g^3_{k3})$, $r_G \in E_x(g^2_{k2})$, and $r_I \in E_x(g^1_{k1})$.

Now we define the following intervals.

1) $I_a = [r_{\text{en}}, r_{\text{ex}}]$ where $r_{\text{en}} \in E_n(g_K)$, $r_{\text{ex}} \in E_x(g_K)$, and $-vr < g_K(r) < vr$ for all $r \in (r_{\text{en}}, r_{\text{ex}})$.
2) $I_b = [r_1, r_2]$ where $-vr \le g_K(r) \le vr$ for all $r \in [r_1, r_2]$ and for all $\delta > 0$ $(r_1 - \delta, r_1) \notin S_K(f)$ and $(r_2, r_2 + \delta) \notin S_K(f)$. Furthermore, there exists at least one $\bar{r} \in [r_1, r_2]$ such that $\bar{r} \in E_t(g_K)$. It is to be noted that either $r_1 \in E_n(g_K)$ or $r_1 \in E_t(g_K)$ and either $r_2 \in E_t(g_K)$ or $r_2 \in E_x(g_K)$.
3) $I_c = [r_{\text{en}}, \infty)$ where $r_{\text{en}} \in E_n(g_K)$ and $-vr < g_K(r) < vr$ for all $r > r_{\text{en}}$.
4) $I_d = [r_1, \infty)$ where $-vr \le g_K(r) \le vr$ for all $r \in [r_1, \infty)$ and for all $\delta > 0$ $(r_1 - \delta, r_1) \notin S_K(f)$. So, either $r_1 \in E_n(g_K)$ or $r_1 \in E_t(g_K)$. Also, there exists at least one $\bar{r} \ge r_1$ such that $\bar{r} \in E_t(g_K)$.
5) $I_e = [r_{t1}, r_{t2}]$ where $[r_{t1}, r_{t2}] \in E_t(g_K)$ and for all $\delta > 0$ such that $(r_{t1} - \delta, r_{t1}) \notin \mathcal{S}_K$ and $(r_{t2}, r_{t2} + \delta) \notin \mathcal{S}_K$.

Example: In Fig. 3, $[r_A, r_I]$ for $g^1_{k1}(r)$ and $[r_D, r_E]$ for $g^3_{k3}(r)$ are of the form I_a. $g^2_{k2}(r)$ has $[r_B, r_G]$ of the form I_b. $g^3_{k3}(r)$ with $[r_F, \infty)$ of the form I_c. Form I_d is shown through $g^3_{k4}(r)$ with the interval $[r_H, \infty)$. I_c is shown using $g^5_{k5}(r)$, which has a singleton set $\{r_C\}$.

In the next section, we use these terminologies to analyze the behavior of the unicycle under input (2).

IV. Analysis of the Trajectories

In this section, we study the trajectories of the unicycle and the instantaneous variation of r and ϕ under the input (2).

To start with, we discuss some results derived from the definitions of $g_K(r)$ and $\mathcal{S}_K(f)$ that are useful for further analysis.

1) For any given $f(r)$ and K, any interval $I \subseteq \mathcal{S}_K(f)$ is of any one of the forms $I_a, I_b, \ldots, I_e$ and is disjoint of the others. Thus, $\mathcal{S}_K(f)$ comprises of the disjoint union of intervals of the forms I_a, $I_b, \ldots, I_e$.

Example: For $f(r) = -\frac{0.375\pi \sin(1.5\pi r)}{r}$ and $K = k3 = 2.14$, $g_K(r) = 2.14 + 0.25\cos(1.5\pi r)$ and $\mathcal{S}_K(f) = I_1 \bigcup I_2$ where $I_1 = [4.52, 5]$ and $I_2 = [5.47, \infty]$ are disjoint of each other. This particular $g_K(r)$ is shown in Fig. 3 as $g^3_{k3}(r)$ with $r_D = 4.52$, $r_E = 5$, and $r_F = 5.57$.

2) When $f(r)$ is fixed, $\mathcal{S}_K(f)$ varies with the variation of K.

Example: For the same $f(r)$ as discussed in the previous point, $K = k4 = -0.575$ gives $g^3_{k4}(r) = -0.575 + 0.25\cos(1.5\pi r)$ with $\mathcal{S}_K(f) = [r_H, \infty)$ where $r_H = 4.3$, which is of the form I_d with a tangent point at $r = 1.95$ as illustrated in Fig. 3.

3) Certain values of K may render $\mathcal{S}_K(f) = \emptyset$. This means that (6) will not hold for any combination of $r \in (0, \infty)$ and $\phi \in [0, 2\pi)$ for given $f(r)$ and K.

Example: When $f(r) = (-2r + 1)/r$, $\tilde{f}(r) = -r^2 + r$. As shown in Fig. 3. $K = k1 = 1$ gives $g^1_{k1}(r) = -r^2 + r + 1$ that has $\mathcal{S}_K(f) = [r_C, r_F] = [1.326, 1.943]$. However, as K changes to $k6 = -1.25$, $g^1_{k6}(r) = -r^2 + r - 1.25$, and $\mathcal{S}_K(f) = \emptyset$.

4) Suppose $f(r)$ and K are specified. Any $r \in \mathcal{S}_K(f)$ satisfies (6) and, hence, is a candidate value of r_0. (5) gives two possibilities for ϕ_0, out of which either one can be chosen. On the other hand, when $f(r)$ and (r_0, ϕ_0) are specified, K is given by (5). The value of K changes as initial conditions change.
5) Given only $f(r)$, the range of values of K is calculated over $r_0 \in (0, \infty)$ and $\phi \in [0, 2\pi)$ by using (5). For example, the range of K for $f(r) = \eta r$ is detailed in [22] where η is a real constant.
6) Given $f(r)$, there always exists at least one value of K such that $\mathcal{S}_K(f) \neq 0$. This is because $g_K(r) = \tilde{f}(r) - K$ gives the following three possibilities: (a) There exists at least one r such that $-vr \le \tilde{f}(r) \le vr$. Then, $r \in \mathcal{S}_0(f)$ and hence $\mathcal{S}_K(f) \neq 0$ for $K = 0$. (b) Let $\tilde{f}(r) > vr$ for all $r \ge 0$. We pick any $r_1 > 0$ and set $K = \tilde{f}(r_1) - vr_1$. Then, $g_K(r_1) = vr_1$ and so $\mathcal{S}_K(f) \neq 0$. (c) Suppose $\tilde{f}(r) < -vr$ $\forall r \ge 0$. Similar to the previous case, we pick $r_2 > 0$ and set $K = \tilde{f}(r_2) + vr_2$, which will ensure $\mathcal{S}_K(f) \neq 0$.

Now, we discuss some more properties of entry, exit, and tangential points.

Remark 1: The solution set of (6) corresponds to the intersection of $g_K(r)$ with $(-v\sin\phi)r$. For any value of ϕ, $(-v\sin\phi)r$ represents a straight line with respect to r passing through origin with slope $-v\sin\phi$ as shown in dotted lines in Fig. 3. So using (6), the intersection of $g_K(r)$ with $\pm vr$ yields $\phi \in \{\frac{\pi}{2}, \frac{3\pi}{2}\}$. At an intersection point of $g_K(r)$ with vr (that is, $\phi = \frac{3\pi}{2}$), the slope of $g_K(r)$ is less than v for an entry point, equal to v at a tangential point and greater than v at an exit point. Similar argument holds for intersection with $-vr$ (that is, $\phi = \frac{\pi}{2}$). Therefore, in (6), $\phi \in \{\frac{\pi}{2}, \frac{3\pi}{2}\}$ only at entry, exit, and tangential points.

Next, we study the trajectory of the unicycle in different intervals of $\mathcal{S}_K(f)$.

A. Characterization of the Trajectories

For any $f(r)$ and K, the trajectory of the unicycle depends on the form of the intervals of $\mathcal{S}_K(f)$ and the interval in which the initial conditions (r_0, ϕ_0) lie.

To start with, an analysis on tangential points is presented. Any tangential point bears a special property of stationarity with respect to (3), which implies that whenever instantaneous $r \in E_t(g_K)$, r does not change thereafter. Lemma 1 illustrates this property.

Lemma 1: Given any $f(r)$ and K, if instantaneous $r(t) = \bar{r}$ at any time $t_1 \ge 0$ where $\bar{r} \in E_t(g_K)$, then the unicycle trajectory becomes circular with radius $\bar{r}$ for all $t \ge t_1$.

Proof: Since $\bar{r} \in E_t(g_K)$, then from (10) if we consider $g_K(\bar{r}) = v\bar{r}$ and $\frac{d}{dr}g_K(r) = v$, then $f(\bar{r}) = \frac{1}{r}\frac{d}{dr}g_K(r) = \frac{v}{\bar{r}}$ and from (6), $\phi|_{r=\bar{r}} = \phi_{\bar{r}} = \frac{3\pi}{2}$. This implies from (3) that

$\dot{r} = 0$ and $\dot{\phi} = 0$. Then, all the other higher derivatives of r and ϕ are nullified. Similar arguments hold when $g_K(\bar{r}) = -v\bar{r}$ and $\frac{d}{dr} g_K(r) = -v$. Thus, if $r(t_1) = \bar{r}$ at time $t_1 > 0$, then $r(t) = \bar{r}$ for all time $t \geq t_1$. However, $\dot{\alpha} = f(\bar{r}) = \pm\frac{v}{\bar{r}}$ and $\dot{\theta} = -\frac{v \sin \phi_{\bar{r}}}{\bar{r}} \neq 0$ become constant. Hence, the unicycle starts moving in a circular trajectory with radius $\bar{r}$. ■

For Lemma 1 to hold, the initial trajectory of the unicycle need not be circular. This implies $r_0 \in E_t(g_K)$ is not mandatory. However, once $r(t) = \bar{r}$ starting from some r_0, the unicycle starts moving on a circle of radius $\bar{r}$ where $\bar{r} \in E_t(g_K)$. Next we try to find how $r(t)$ varies with time and the values it takes for the different forms of the intervals of $\mathcal{S}_K(f)$.

Lemma 2: Given any $f(r)$ and K, let $I \subseteq \mathcal{S}_K(f)$ have any one of the forms $I_a, I_b, \ldots, I_e$. If $r(0) \in I$, then instantaneous $r(t) \in I$ for all $t \geq 0$.

Proof: This can be proved by showing the bounds of $r(t)$. In order to investigate the extrema of r, we set $\dot{r} = 0$ in (3) which gives $\phi \in \{\frac{\pi}{2}, \frac{3\pi}{2}\}$. As explained in Remark 1, the corresponding values of r could be either entry, exit, or tangential points. Now, at any entry point r_{en}, if $\phi = \frac{3\pi}{2}$, then from (6) and (9) $\frac{d}{dr} g_K(r) < v$. Using (3) and definition of $g_K(r)$, we get $\dot{\phi} = \frac{\frac{d}{dr} g_K(r) - v}{r} < 0$. So from (3) $\ddot{r} = v \sin\phi\dot{\phi} > 0$. Hence, $r(t)$ is minimum at $r = r_{\text{en}}$. It can be similarly shown for $\phi = \frac{\pi}{2}$ that $\min(r(t)) = r_{\text{en}}$. At any exit point r_{ex}, if $\phi = \frac{3\pi}{2}$, then from (6) and (11), $\frac{d}{dr} g_K(r) > v$, $\dot{\phi} = \frac{\frac{d}{dr} g_K(r) + v}{r} > 0$ implying $\ddot{r} < 0$. So $\max(r(t)) = r_{\text{ex}}$. We get the same result when $\phi = \frac{\pi}{2}$. Now, we analyze the behavior of $r(t)$ in different forms of I.

Suppose $I = [r_{\text{en}}, r_{\text{ex}}]$ is of the form I_a. By the very nature of entry and exit points, $\max(r(t)) = r_{\text{ex}}$ and $\min(r(t)) = r_{\text{en}}$. So $r(t) \in I$ and is bounded below and above by r_{en} and r_{ex}, respectively, which implies $r(t) \in I$ for all time $t \geq 0$.

Let $I = [r_1, r_2]$ be of the form I_b. If $r_1 \in E_n(g_K)$, then $\min(r(t)) = r_1$. If $r_1 \in E_t(g_K)$, then using Lemma 1, whenever $r(t) = r_1$ at $t = t_1 > 0$, $r(t) = r_1$ for all $t > t_1$. This implies that $r(t) \geq r_1$ for all time $t \geq 0$. Similarly, it can be shown that $r(t) \leq r_2$ for all $t \geq 0$. Hence, $r(t) \in I$ for all time $t \geq 0$.

When $I = [r_{\text{en}}, \infty)$ is of the form I_c, $r_{\text{en}} \in E_n(g_K)$, and $\min(r(t)) = r_{\text{en}}$. This implies $r(t) \geq r_{\text{en}}$ and, hence, $r(t) \in I$ for all time $t \geq 0$.

Suppose $I = [r_1, \infty)$ is of the form I_d. Following the analysis for r_1 when I is of the form I_b, we find that $r(t) \geq r_1$ for all time $t \geq 0$. Hence, $r(t) \in I$ for all time $t \geq 0$.

Let I be of the form I_e. Then, using Lemma 1, $r(t) = r(0) \in I$ for all $t \geq 0$ as $r(0) \in E_t(g_K)$. ■

This shows that $r(t)$ is bounded within I for all of its different forms whenever $r_0 \in I$. Now we analyze the variation of both $r(t)$ and the unicycle trajectory within I.

Theorem 1: If a unicycle with kinematics (1) and control (2) has initial condition (r_0, ϕ_0) such that $r_0 \in I$ where $I \subseteq \mathcal{S}_K(f)$ has any one of the forms $I_a, I_b, \ldots, I_e$, then its trajectory is

1) periodic in (r, ϕ) and annular pattern if
   a) I has the form I_a
2) an unbounded pattern if
   a) I has the form I_c or
   b) I has the form I_d with $\bar{r} < r_0$ for all $\bar{r} \in E_t(g_K)$ and $\phi_0 \in (\frac{\pi}{2}, \frac{3\pi}{2})$
3) circular pattern if
   a) I has the form I_b or
   b) I has the form I_d with $\phi_0 \in (-\frac{\pi}{2}, \frac{\pi}{2})$ or
   c) I has the form I_d with $\phi_0 \in (\frac{\pi}{2}, \frac{3\pi}{2})$ and at least one $\bar{r} > r_0$ such that $\bar{r} \in E_t(g_K)$ or
   d) I has the form I_e.

Proof: When $f(r)$ and (r_0, ϕ_0) are given, K is given by (5). Since $r = r_0$ and $\phi = \phi_0$ satisfy (4), $r_0 \in I \subseteq \mathcal{S}_K$. Now we show the behavior of the unicycle within I for each of its possible form.

Suppose $I = [r_{\text{en}}, r_{\text{ex}}]$ is of the form I_a. As proved in Lemma 2, $\max(r(t)) = r_{\text{ex}}$ and $\min(r(t)) = r_{\text{en}}$. Remark 1 shows that $\phi \in \{\frac{\pi}{2}, \frac{3\pi}{2}\}$ only at entry, exit, and tangential points. Hence, $\phi \notin \{\frac{\pi}{2}, \frac{3\pi}{2}\}$ for $r \in (r_{\text{en}}, r_{\text{ex}})$. Since there are no entry, exit, and tangential points in $(r_{\text{en}}, r_{\text{ex}})$, there are no local extrema of $r(t)$ in $(r_{\text{en}}, r_{\text{ex}})$ (as (3) shows that $\dot{r} \neq 0$). Thus, $r(t)$ either increases monotonically from r_{en} to r_{ex} or decreases monotonically from r_{ex} to r_{en}.

Using (7) in (3) gives $r\dot{\phi} = \frac{d}{dr} g_K(r) + v \sin\phi$. Furthermore, (9) and (11) suggest that $\dot{\phi} \neq 0$ at r_{en} and r_{ex}. By the continuity property of ϕ and $\dot{\phi}$, there exist intervals $[r_{\text{en}}, r_{\text{en}} + \epsilon_1)$ and $(r_{\text{ex}} - \epsilon_2, r_{\text{ex}}]$ in which $\phi \neq \{0, 2\pi\}$ and $\dot{\phi} \neq 0$. Here, $\epsilon_1, \epsilon_2 > 0$ are chosen such that $r_{\text{ex}} - \epsilon_2 > r_{\text{en}} + \epsilon_1$. This divides $[r_{\text{en}}, r_{\text{ex}}]$ in three subintervals: $[r_{\text{en}}, r_{\text{en}} + \epsilon_1)$, $[r_{\text{en}} + \epsilon_1, r_{\text{ex}} - \epsilon_2]$, and $(r_{\text{ex}} - \epsilon_2, r_{\text{ex}}]$. In $[r_{\text{en}}, r_{\text{en}} + \epsilon_1)$ and $(r_{\text{ex}} - \epsilon_2, r_{\text{ex}}]$, $\ddot{r} = v \sin\phi\dot{\phi} \neq 0$ as $\dot{\phi} \neq 0$ and $\sin\phi \neq 0$. This implies that $\ddot{r}$ does not change sign in these intervals. Then, the absolute rate of change of $\dot{r}$ is lower bounded by $\ddot{r}_{\min} = \min|\ddot{r}| > 0$. This ensures that both $\dot{r}$ and r traverse $[r_{\text{en}}, r_{\text{en}} + \epsilon_1)$ and $(r_{\text{ex}} - \epsilon_2, r_{\text{ex}}]$ in finite time. Now in $[r_{\text{en}} + \epsilon_1, r_{\text{ex}} - \epsilon_2]$, $\dot{r} \neq 0$. Let $\dot{r}_{\min} = \min|\dot{r}|$. Then, this region is traversed in time $t \leqslant (r_{\text{ex}} - \epsilon_2 - r_{\text{en}} - \epsilon_1)/\dot{r}_{\min}$. Thus, $[r_{\text{en}}, r_{\text{ex}}]$ is always traversed by the unicycle in finite time.

Now, let us suppose at $t = t_1$, $(r(t_1), \phi(t_1)) = (r_{ex}, \bar{\phi}_1)$ where $\bar{\phi}_1 \in \{\frac{\pi}{2}, \frac{3\pi}{2}\}$. Using (4), $K = \tilde{f}(r_{\text{ex}}) + v r_{\text{ex}} \sin\bar{\phi}_1$. Since $\max(r(t)) = r_{\text{ex}}$, $r(t)$ starts decreasing till it reaches r_{en}. Then ϕ becomes $\bar{\phi}_2$ where again $\bar{\phi}_2 \in \{\frac{\pi}{2}, \frac{3\pi}{2}\}$. Again, after time $t = t_1 + T$, $r(t)$ increases to r_{ex} and ϕ becomes $\bar{\phi}_3$. From (4), $K = \tilde{f}(r_{\text{ex}}) + v r_{\text{ex}} \sin\bar{\phi}_1 = \tilde{f}(r_{\text{ex}}) + v r_{\text{ex}} \sin\bar{\phi}_3$, which implies $\bar{\phi}_1 = \bar{\phi}_3$. Thus, unicycle returns to the initial condition $(r_{\text{ex}}, \bar{\phi}_1)$ after T units of time. Since the unicycle follows the same kinematics (1) from there, after another T units of time, it returns to (r_{ex}, ϕ_1) resulting in a trajectory that is annular and periodic in (r, ϕ).

When $I = [r_1, r_2]$ is of the form I_b with $r_1 \in E_n(g_K)$ and $r_2 \in E_x(g_K)$, then $r(t)$ will vary as in the previous case until it encounters some $\bar{r} \in E_t(g_K)$. If either or both $r_1, r_2 \in E_t(g_K)$, then $r(t)$ will vary as in the previous case in (r_1, r_2). If it encounters some $\bar{r} \in E_t(g_K)$ in between, then the trajectory will become circular. Else, trajectory becomes circular once $r(t)$ reaches either r_1 or r_2. Hence, we always get a circular trajectory.

Let $I = [r_{\text{en}}, \infty)$ be of the form I_c. When $\phi_0 \in (\frac{\pi}{2}, \frac{3\pi}{2})$, then from (3), $\dot{r} > 0$ initially. So $r(t)$ increases monotonically from

r_0 to ∞. Similarly when $\phi_0 \in (-\frac{\pi}{2}, \frac{\pi}{2})$, $\dot{r} < 0$, $r(t)$ reduces monotonically from r_0 to r_{en}. r_{en} being an entry point, as proved in Lemma 2, $\min(r(t)) = r_{\text{en}}$ so $r(t)$ increases monotonically to ∞. Thus, trajectory is unbounded.

Suppose $I = [r_1, \infty)$ is of the form I_d. If $\phi_0 \in \left(\frac{\pi}{2}, \frac{3\pi}{2}\right)$, then $\dot{r} > 0$ initially. Therefore, $r(t)$ increases monotonically. If $\bar{r} < r_0$ for all $\bar{r} \in E_t(g_K)$, then $r(t)$ goes to ∞ and trajectory becomes unbounded. Else from Lemma 1, we get a circular pattern. If $\phi_0 \in \left(-\frac{\pi}{2}, \frac{\pi}{2}\right)$, then $\dot{r} < 0$. Since $r(t)$ is monotonically decreasing, if there is any $\bar{r} \in E_t(g_K)$ in $[r_1, r_0)$, then from Lemma 1, the trajectory is circular. Else $r_1 \in E_n(g_K)$ and $\min(r(t)) = r_1$. Once r_1 is reached, $r(t)$ increases monotonically to a tangential point. Hence, the trajectory becomes circular.

For I of the form I_e, the trajectory of unicycle is circular as every $r_0 \in I$ belongs to $E_t(g_K)$. ■

We infer from the proof of Theorem 1 that for any $f(r)$ and K, irrespective of the form of the interval, it is guaranteed that the minimum and maximum value of instantaneous $r(t)$ occur at entry point r_{en} and exit point r_{ex} unless $r(t)$ gets trapped at any tangential point. Henceforth, we refer to the maximum value of r as $R_{\max}$ and minimum value as $R_{\min}$. Similarly, the unicycle trajectory is unbounded when $R_{\max}$ does not exist implying I is unbounded ($[r_{\text{en}}, \infty)$).

We already know that for any given $f(r)$ and K, $\mathcal{S}_K(f)$ can have multiple subsets. Then, the pattern generated by the unicycle depends on the subset I for which $r_0 \in I$. Keeping $f(r)$ fixed and altering r_0 such that it belongs to different intervals I results in different patterns in each case. Furthermore, Lemma 2 ensures that once we choose r_0 in some interval, it cannot migrate to any other interval.

Examples:

Case 1: Consider $f(r) = 2/r$, $(r_0, \phi_0) = (4, 270^\circ)$ and $v = 1$. From (5), $K = 4$ and $g_4(r) = 2r - 4$. Here, $S_4(2/r) = [1.33, 4]$ is of the form I_a as shown in Fig. 4(a). The trajectory of the unicycle is annular and periodic as shown in Fig. 1(a).

Case 2: Let $f(r) = 1/r$, $(r_0, \phi_0) = (2.5, 90^\circ)$ and $v = 1$. Then using (5), $K = 5$ and $g_5(r) = r - 5$. $S_5(1/r) = [2.5, \infty)$ which is of the form I_c as shown in Fig. 4(b). The trajectory of the unicycle is unbounded as shown in Fig. 1(b).

Case 3: Let $f(r) = 0.25r$, $(r_0, \phi_0) = (2, 270^\circ)$ and $v = 1$. Then using (5), $K = -4/3$ and $g_K(r) = 0.25r^3/3 + 4/3$. $S_5(1/r) = 2$, which is of the form I_e as shown in Fig. 4(c). The trajectory of the unicycle is circular as shown in Fig. 4(d).

Given any $f(r)$ and (r_0, ϕ_0), we know that if $r(t) \in I \subseteq \mathcal{S}_K$ where I has any one of the forms I_a or I_b (that is I is compact), then there exists $r_1 = \min(\arg\max(-\frac{g_K(r)}{vr}))$ and $r_2 = \min(\arg\min(-\frac{g_K(r)}{vr}))$ for all $r \in I$. Then, using (6), we can write for all $r(t) \in I$

$$\phi(t) \in \left[-\sin^{-1}\left(\frac{g_K(r_2)}{r_2}\right), -\sin^{-1}\left(\frac{g_K(r_1)}{r_1}\right)\right] \cup \left[\pi + \sin^{-1}\left(\frac{g_K(r_1)}{r_1}\right), \pi + \sin^{-1}\left(\frac{g_K(r_2)}{r_2}\right)\right]. \tag{12}$$

The analysis for noncompact intervals I having the form I_c or I_d can be extended in a similar manner. For each instantaneous r, $\sin\phi$ is uniquely given by (6). This implies that ϕ can take two possible values, ϕ and $\pi - \phi$. Depending on whether ϕ is acute or obtuse, $\dot{r}$ is positive in one case and negative in the other, except in the extremum values of r where $\dot{r} = 0$. This emphasizes the periodic nature of r.

The analysis carried out so far assumes a given K. Now for a given $f(r)$, if K varies, $g_K(r)$ varies in accordance because $g_K(r) = \tilde{f}(r) - K$. Hence, the entry, exit, and tangential points for $g_K(r)$ and the intervals $\mathcal{S}_K(f)$ also vary.

K can be expressed in terms of $R_{\max}$, $R_{\min}$, and $f(r)$ as follows: Since $\phi \in \{\frac{\pi}{2}, \frac{3\pi}{2}\}$ at $R_{\max}$ and $R_{\min}$, we get two conditions $\tilde{f}(R_{\max}) - \tilde{f}(R_{\min}) = v|R_{\max} - R_{\min}|$ and $\tilde{f}(R_{\max}) - \tilde{f}(R_{\min}) = v|R_{\max} + R_{\min}|$. Substitution of these conditions in (4) leads to two values of K given by

$$K = \begin{cases} \frac{R_{\max}\tilde{f}(R_{\max}) + R_{\min}\tilde{f}(R_{\min})}{R_{\max} + R_{\min}} & |\tilde{f}(R_{\max}) - \tilde{f}(R_{\min})| = v(R_{\max} + R_{\min}) \\ \frac{R_{\max}\tilde{f}(R_{\max}) - R_{\min}\tilde{f}(R_{\min})}{R_{\max} - R_{\min}} & |\tilde{f}(R_{\max}) - \tilde{f}(R_{\min})| = v(R_{\max} - R_{\min}) \end{cases}. \tag{13}$$

From (13), it is obvious that $K = 0$ only when $\tilde{f}(R_{\max})R_{\min} = \pm\tilde{f}(R_{\min})R_{\max}$.

The (r, ϕ) profile and, hence, the unicycle trajectory depend on $g_K(r)$. Now if $R_{\max}$, $R_{\min}$, and $f(r)$ are given, the possibility of generation of annular pattern is discussed next.

Corollary 1: A unicycle with kinematics (1) and control (2) can trace an annular pattern of radii $R_{\max}$ and $R_{\min}$ with $R_{\max} \geq R_{\min} \geq 0$ if and only if

a) $[R_{\min}, R_{\max}] \subseteq \mathcal{S}_K(f)$ is of the form I_a

and initial conditions (r_0, ϕ_0) are selected as follows

b) $r_0 \in [R_{\min}, R_{\max}]$

c) $\phi_0 \in \{\pi + \sin^{-1}(\frac{g_K(r_0)}{vr_0}), -\sin^{-1}(\frac{g_K(r_0)}{vr_0})\}$.

where K is obtained from (13).

Proof: Given $R_{\max}$, $R_{\min}$, and $f(r)$, (13) gives the possible values of K. If $[R_{\min}, R_{\max}] \subseteq S_K(f)$ and is of the form I_a, then from Theorem 1, we can get an annular pattern provided appropriate initial conditions are selected. Lemma 2 shows that in order to generate a pattern in $[R_{\min}, R_{\max}]$, we need to ensure $r_0 \in [R_{\min}, R_{\max}]$ which is true from condition (b). From condition (c), ϕ_0 satisfies (6). Hence, we get an annular pattern.

Now, for the sufficient condition, suppose the unicycle traces the annular pattern when $R_{\max}$, $R_{\min}$, and $f(r)$ are given. Then, Theorem 1 shows that $[R_{\min}, R_{\max}] \subseteq S_K(f)$ is of the form I_a. To generate the pattern in $[R_{\min}, R_{\max}]$, Lemma 2 demands $r_0 \in [R_{\min}, R_{\max}]$ and ϕ_0 is selected using (6), which are given in conditions (b) and (c). ■

When condition (a) of Corollary 1 does not hold for the value of K obtained from (13), we infer from Corollary 1 that the unicycle cannot generate the desired annulus. In such a case, any of $f(r)$, $R_{\max}$, or $R_{\min}$ needs to be changed.

V. Designing Control to Generate Annular Trajectories

In the previous section, we found the pattern that gets generated and the corresponding $\mathcal{S}_K(f)$ when $f(r)$ is already

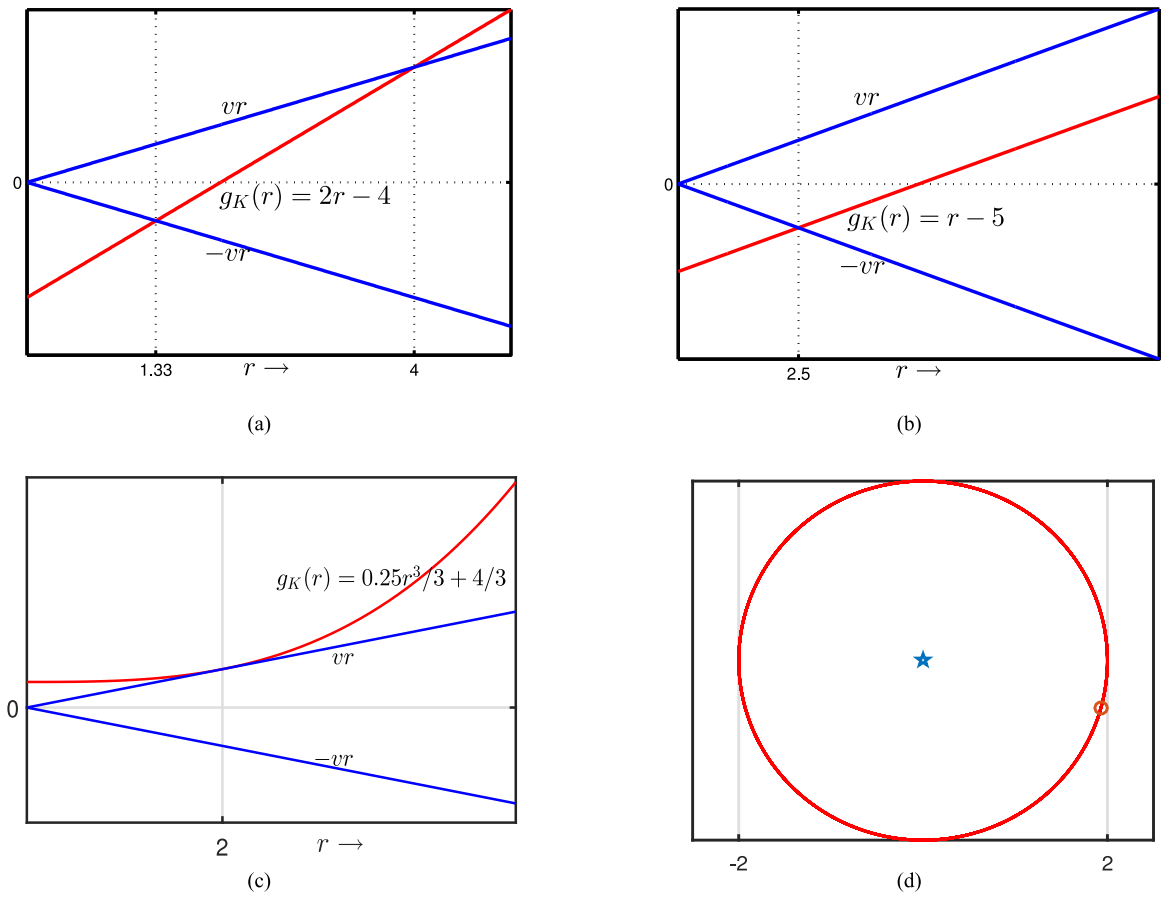

Fig. 4. Examples of $g_K(r)$ s for annular, spiral, and circular patterns. (a) $g_K(r) = 2r - 4$. (b) $g_K(r) = r - 5$. (c) $g_K(r) = 0.25r^3/3 + 4/3$. (d) Circular trajectory.

specified. On the contrary, in this section, we generate a desired pattern by designing $f(r)$.

A. Designing the Control Input $f(r)$

We begin by explaining the conditions that are required for generating any annular pattern.

Theorem 2: A unicycle with kinematics (1) and control (2) generates an annular pattern of radii $R_{\max}$ and $R_{\min}$, with $R_{\max} > R_{\min} \geq 0$, if and only if the control input is $f(r) = \frac{1}{r}\frac{dg(r)}{dr}$ where $g(r)$ satisfies,

a) $g(r) \in C^1$ for all $r \in [R_{\min}, R_{\max}]$,
b) $-vr < g(r) < vr$ for all $r \in (R_{\min}, R_{\max})$,
c) $g(R_{\min}) = \pm vR_{\min}$,
d) $g(R_{\max}) = \pm vR_{\max}$,
e) $\frac{d}{dr}g(r) \mid_{r \in \{R_{\min}, R_{\max}\}} \neq \pm v$.

Furthermore, if ϕ_0 is specified, then $g(r)$ should also satisfy

f) $g(r_0) = -vr_0 \sin\phi_0$

where r_0 may be specified or chosen such that,

g) $r_0 \in [R_{\min}, R_{\max}]$.

Proof: Suppose there exists a function $g(r)$ that satisfies conditions $(a) - (e)$ of Theorem 2. Condition (a) implies the existence of a continuous function $f(r)$ obtained using (7). (13) gives the value of K using $R_{\max}$, $R_{\min}$, and $f(r)$. Using (8), condition (b) implies $(R_{\min}, R_{\max}) \subset S_K(f)$ and there does not exist any tangent point in $(R_{\min}, R_{\max})$. From condition (c), at $r = R_{\min}$, if $g(R_{\min}) = vR_{\min}$, then $\frac{d}{dr}g(r) \mid_{r=R_{\min}} < v$ or if $g(R_{\min}) = -vR_{\min}$, then $\frac{d}{dr}g(r) \mid_{r=R_{\min}} > -v$ such that condition (b) is not violated. Similarly, from condition (d), at $r = R_{\max}$, $g(R_{\max}) = vR_{\max}$ implies $\frac{d}{dr}g(r) \mid_{r=R_{\max}} > v$ and $g(R_{\max}) = -vR_{\max}$ implies $\frac{d}{dr}g(r) \mid_{r=R_{\max}} < -v$. Using condition (e), we get $R_{\min} \in E_n(g)$ and $R_{\max} \in E_x(g)$. This ensures that $[R_{\min}, R_{\max}] \subseteq \mathcal{S}_K(f)$ is of the form I_a. The choice of (r_0, ϕ_0) using $(f) - (g)$ ensures $r \in [R_{\min}, R_{\max}]$ for all time by invoking Lemma 2. Thus, from Theorem 1, we get an annular trajectory starting from (r_0, ϕ_0) with $\min(r(t)) = R_{\min}$ and $\max(r(t)) = R_{\max}$.

On the other hand, suppose that the agent trajectory is an annulus of radii $R_{\min}$ and $R_{\max}$. Theorem 1 shows that $I = [R_{\min}, R_{\max}]$ is of the form I_a for the corresponding $g_K(r)$, which satisfies conditions $(a) - (e)$. Then, the desired input is calculated using (7). Then r_0 is calculated from Lemma 2 such that $r_0 \in I$. Since (r_0, ϕ_0) must be a point on the pattern, ϕ_0 is chosen such that (6) holds. ■

The conditions (a)–(e) in Theorem 2 pertain to the design of $g_K(r)$ such that the desired annulus is guaranteed. The corresponding $\mathcal{S}_K$ may even have multiple subsets. When $I = [R_{\min}, R_{\max}] \subsetneq \mathcal{S}_K$, not every $r \in \mathcal{S}_K$ is a candidate r_0

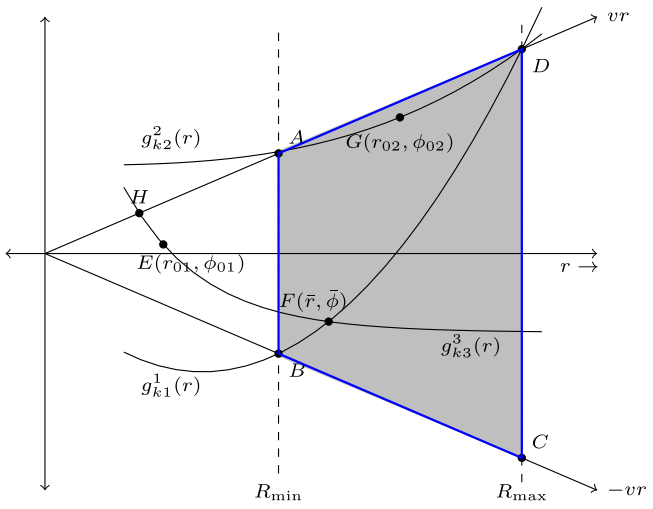

Fig. 5. Feasible region for $g(r)$: Trapezium.

and the range of r_0 is reduced from $\mathcal{S}_K$ to I as indicated in condition (f) of Theorem 2. Conditions (f) and (g) guarantee that (r_0, ϕ_0) satisfies (4) and represents a point on the pattern.

Remark 2: The conditions in Theorem 2 are shown graphically in Fig. 5 . Consider the trapezium $ABCD$ formed by the lines $\pm vr$, $r = R_{\min}$ and $r = R_{\max}$. Condition (b) requires any $g(r)$ function to be within $\pm vr$. Condition (c) and (d) imply that any $g(r)$ must pass through either A or B at $r = R_{\min}$ and C or D at $r = R_{\max}$, respectively. Combining these conditions, we infer that any curve within the trapezium $ABCD$ that passes through vertices A or B and C or D is a candidate function for $g(r)$. If specified, the initial condition (r_0, ϕ_0) must lie on $g(r)$ as given by conditions (f) and (g). There can be infinitely many $g(r)$ functions that satisfy these conditions resulting in infinitely many distinct annular patterns with radii $R_{\min}$ and $R_{\max}$. Fig. 5 shows feasible candidate functions for $\max(r) = R_{\max}$ and $\min(r) = R_{\min}$ as $g^1_{k1}(r)$ and $g^2_{k2}(r)$ that are bounded in the trapezium $ABCD$.

Next, we present an example to illustrate Theorem 2.

Example: Suppose $R_{\max} = 6$, $R_{\min} = 3$, and $v = 3/7$. In reference to Fig. 5, $g^1_{k1}(r) = 0.25r^2 - r - 0.5$ is designed such that $g^1_{k1}(R_{\max}) = 2.5$, $g^1_{k1}(R_{\min}) = -1.25$ and $g^1_{k1}(r) \in (-vr, vr)$ for all $r \in (3, 6)$ satisfying conditions (a)–(e) of Theorem 2. Then, $f_1(r) = 0.5 - 1/r$. We select $F(r_0 = \bar{r}, \phi_0 = \bar{\phi})$ as the initial condition lying on $g^1_{k1}(r)$. However, if $\phi_0 = \phi_{02}$ is specified, then r_0 is chosen as the intersection point of $(-v \sin\phi_{02})r$ line and $g^1_{k1}(r)$. If $r_0 = r_{02}$ is specified as some other value, then obviously we cannot use $g^1_{k1}(r)$. So, we select $G(r_0 = r_{02}, \phi_0 = \phi_{02})$ and design $g^2_{k2}(r) = 0.02r^3/3 + 1.1184$ that satisfies conditions (a)–(g) of Theorem 2. The corresponding input is $f_2(r) = 0.02r$. The unicycle trajectories generated with inputs $f_1(r)$ and $f_2(r)$ are shown in Fig. 7(x) and (a), respectively.

B. Designing a Switching Control Strategy

Theorem 2 gives the conditions for designing $f(r)$ such that the unicycle traces the desired pattern. Suppose both r_0 and ϕ_0 are specified, Theorem 2 takes them into account while designing $f(r)$. However, when either or both r_0 and ϕ_0 are not given, then we need to find them. So we discuss next how to find the initial conditions when $f(r)$ is designed using Theorem 2.

Finding the initial conditions (r_0, ϕ_0).

i) If r_0 and ϕ_0 are not given, since $f(r)$ is either known or designed using conditions $(a) - (e)$ of Theorem 2, use conditions (b) and (c) of Corollary 1 to find (r_0, ϕ_0).
ii) If only ϕ_0 is given, the situation is handled in Theorem 2 in conditions (f) and (g).
iii) If only r_0 is given and condition (b) of Corollary 1 is satisfied, then use condition (c) of Corollary 1 to find ϕ_0.
iv) If only r_0 is given and conditions (b) of Corollary 1 is not satisfied, we propose a switching control strategy.
v) When both r_0 and ϕ_0 are given, but $f(r)$ is either given or designed such that conditions (f) and (g) of Theorem 2 are not satisfied, we propose a switching control strategy.

When only $f(r)$, $R_{\min}$, $R_{\max}$ $(R_{\max} \geq R_{\min})$ are given

$$g_K(r) = \tilde{f}(r) - K \tag{14}$$

where $\tilde{f}(r)$ is as defined in (4) and K is given by (13). For both the values of K, $f(r)$ gives the same $R_{\min}$ and $R_{\max}$. Suppose r_0 and ϕ_0 are also given. A switching control strategy is proposed to take care of initial conditions when they do not satisfy conditions (b) and (c) of Corollary 1. This can happen in practical situations in which the initial position of the agent might be constrained to be away from the desired pattern (for example, monitoring any remote area) or bear only a limited range of heading angles. Such situations refer to cases (iv) and (v) above. So when (r_0, ϕ_0) is not a point on the pattern, we propose the switching strategy presented in Theorem 3.

Theorem 3: Given $f(r)$, r_0, ϕ_0, $R_{\min}$, and $R_{\max}$ with $R_{\max} > R_{\min} \geq 0$ such that condition (a) of Corollary 1 holds, but either or both of conditions (b) and (c) do not hold. Consider a function $g^i(r)$ in a region $[R_1, R_2]$ with $R_2 > R_1 > 0$ such that

a) $R_1 \begin{cases} = r_0 & \phi_0 = \pm\frac{\pi}{2} \text{ and } r_0 < R_{\min} \\ < \min\{r_0, R_{\min}\} & \text{otherwise} \end{cases}$

b) $R_2 \begin{cases} = r_0 & \phi_0 = \pm\frac{\pi}{2} \text{ and } r_0 > R_{\max} \\ > \max\{r_0, R_{\max}\} & \text{otherwise.} \end{cases}$

If $g^i(r)$ satisfies conditions (a)–(e) of Theorem 2 in $[R_1, R_2]$ and the following,

c) $g^i(r_0) = -vr_0 \sin\phi_0$,
d) for any $\bar{r} \in [R_1, R_2]$, $g^i(\bar{r}) = g_K(\bar{r})$ where $g_K(r)$ is given by (14),

then, the unicycle generates an annular pattern in $[R_{\min}, R_{\max}]$ from (r_0, ϕ_0) by using the control input

$$u(t) = \begin{cases} f_i(r) & t < \bar{t} \\ f(r) & t \geq \bar{t} \end{cases}$$

$f_i(r) = r^{-1} dg^i(r)/dr$ and $\bar{t}$ denotes the time when $r(t) = \bar{r}$ for the first time.

Proof: Given $R_{\max}$, $R_{\min}$, and $f(r)$, in order to generate the desired pattern, $f(r)$ must satisfy condition (a) of Corollary 1. Since (r_0, ϕ_0) violates either or both of conditions (b) and (c)

Algorithm 1: Switching Control Strategies.

Input: r_0, ϕ_0, $R_{\min}$, $R_{\max}$, $f(r)$
Output: $f_i(r)$, $\bar{r}$

if condition (a) of Corollary 1 is satisfied by $f(r)$, **then**
  if condition (b) of Corollary 1 is satisfied, **then**
    if condition (c) of Corollary 1 is satisfied, **then**
      $f_i(r) = f(r)$
    else
    if $\phi_0 \in [-\frac{\pi}{2}, \frac{\pi}{2}]$ **then**
      select $\bar{r}$ such that $R_{\min} \leq \bar{r} < r_0$ and find $\bar{\phi}$ from (6)
      set $g^i(\bar{r}) = -v\bar{r}\sin\bar{\phi}$
      set $g^i(r_0) = -vr_0\sin\phi_0$
      design $g^i(r) \in C^1$ in $[\bar{r}, r_0]$ such that $-vr < g^i(r) < vr$ for all $r \in (\bar{r}, r_0)$
    else
      select $\bar{r}$ such that $r_0 < \bar{r} \leq R_{\max}$, find $\bar{\phi}$ from (6) and repeat steps 8–9
      design $g^i(r) \in C^1$ in $[r_0, \bar{r}]$ such that $-vr < g^i(r) < vr$ for all $r \in (r_0, \bar{r})$
    end if
  end if
else
  select $\bar{r}$ such that $\bar{r} \in [R_{\min}, R_{\max}]$, find $\bar{\phi}$ from (6) and repeat steps 8–9
  if $r_0 < R_{\min}$ **then**
    if $\phi_0 \in [\frac{\pi}{2}, \frac{3\pi}{2}]$ **then**
      repeat step 13
    else
      select $r^* < r_0$ and set $g^i(r^*)$ such that $r^* \in E_n(g^i)$
      design $g^i(r) \in C^1$ in $[r^*, \bar{r}]$ such that $-vr < g^i(r) < vr$ for all $r \in (r^*, \bar{r})$
    end if
  else
    if $\phi_0 \in [-\frac{\pi}{2}, \frac{\pi}{2}]$ **then**
      repeat step 10
    else
      select $r^* > r_0$ and set $g^i(r^*)$ such that $r^* \in E_x(g^i)$
      design $g^i(r) \in C^1$ in $[\bar{r}, r^*]$ such that $-vr < g^i(r) < vr$ for all $r \in (\bar{r}, r^*)$
    end if
  end if
end if
use $f_i(r) = \frac{1}{r}\frac{d}{dr}g^i(r)$
else
  $f_i(r)$ does not exist
end if

of Corollary 1, it is not a point on the pattern. So, we plan the trajectory from (r_0, ϕ_0) to a point on the desired pattern by using control $f_i(r)$.

To design $f_i(r)$, first $g^i(r)$ is designed to satisfy Theorem 2 in $[R_1, R_2]$. From conditions (a) and (b), $r_0 \in [R_1, R_2]$. And from conditions (c) and (d), $g^i(r)$ passes through r_0 and $\bar{r}$. Then $f_i(r) = \frac{1}{r}\frac{d}{dr}g^i(r)$. Condition (d) shows that $(\bar{r}, \phi_{r=\bar{r}})$ is a point on both the initial and desired patterns. Since Theorem 1 guarantees that all values in $[R_1, R_2]$ are reached periodically, it is ensured that the unicycle reaches $(\bar{r}, \phi_{r=\bar{r}})$ using $f_i(r)$. Once $(\bar{r}, \phi_{r=\bar{r}})$ is reached, the input is switched to $f(r)$. Hence, proved. ■

Theorem 3 guarantees the generation of any desired pattern from any initial condition. The switching occurs at $(\bar{r}, \bar{\phi})$ that is the intersection of $g(r)$ and $g^i(r)$. $g^i(r)$ is designed in $[R_1, R_2]$, which is of the form I_a. Depending on the initial conditions, $[R_1, R_2]$ could be of other forms also. For example, in Fig. 5 switching is required if $(r_0, \phi_0) = (r_{01}, \phi_{01})$ or (r_{02}, ϕ_{02}) and $g(r) = g^1_{k1}(r)$. $g^i(r)$ can be designed such that it passes through (r_0, ϕ_0) and intersects $g^1_{k1}(r)$ and we denote the point of intersection as $(\bar{r}, \bar{\phi})$. For $(r_0, \phi_0) = (r_{02}, \phi_{02})$, we choose $g^i(r) = g^2_{k2}(r)$ with the point of switching as $D(R_{\max}, 3\pi/2)$ and $[r_A, r_D]$ of the form I_a. For $(r_0, \phi_0) = (r_{01}, \phi_{01})$, we can choose $g^i(r) = g^3_{k3}(r)$ with the point of switching being $F(\bar{r}, \bar{\phi})$ and the interval $[r_H, \infty)$ of the form I_c. Algorithm 1 shows all possible locations of initial conditions with respect to region $[R_{\min}, R_{\max}]$ and the corresponding design of $g^i(r)$.

It is to be noted that any other path planning algorithm could be employed to take the unicycle from (r_0, ϕ_0) to $(\bar{r}, \bar{\phi})$. This particular design strategy of $g^i(r)$ is chosen as it results in aesthetically appealing patterns and goes with the flow of the paper.

The design of $f_i(r)$ using Theorem 3 may result in a discontinuous control input $u(t)$ at the point of switching. We can design $g^i(r)$ such that the continuity of $u(t)$ is maintained at $r = \bar{r}$. For the purpose, $g^i(r)$ has to satisfy one more condition along with Theorem 3

$$\frac{d}{dr}g^i(r) \mid_{r=\bar{r}} = \bar{r}f(\bar{r}).$$

Graphically, this would imply that the tangents of $g^i(r) = g(r)$ are the same at $r = \bar{r}$ where $\bar{r}$ is in reference to Fig. 5.

Example: Suppose we want a pattern with $R_{\max} = 10$ and $R_{\min} = 5$ starting from $(r_0, \phi_0) = (2, 10.8^\circ)$. The control input is designed using Theorem 2 and is given as $f(r) = 1 - 4.5/r$, which has $\tilde{f}(r) = 0.5r^2 - 4.5r$. From (13), $K = -5$ and from (6), we find that $[5, 10] \in \mathcal{S}_K(f)$ and is of the form I_a. However, $r_0 \notin [5, 10]$. Therefore, we need to switch the control input. Let the point of switching be $(\bar{r}, \bar{\phi}) = (7.5, -4.78^\circ)$. Since $\phi_0 \in \{-\frac{\pi}{2}, \frac{\pi}{2}\}$, we design $g^i(r) = 7.4\exp(-r)$ using steps 8, 9, and 13. This gives $f_i(r) = -7.4194e^{-r}/r$. $g^i(r)$ and $g(r)$ are as shown in Fig. 6(a). We find that $g^i(r)$ and $g(r)$ intersect at $r = \bar{r}$. The trajectory of the unicycle is shown in Fig. 6(b) that has $R_{\max} = 9.85$ and $R_{\min} = 4.58$. Because of numerical integration, switching does not occur exactly $r = 7.5$, so there is a mismatch in the desired and achieved values of $R_{\max}$ and $R_{\min}$.

Given an annular pattern, this section details the procedure to design $f(r)$ in interval I of the form I_a. For any pattern other than annular (circular or unbounded), the suitable $f(r)$ can be found by designing $g(r)$ in the appropriate interval I (which is given in Theorem 1).

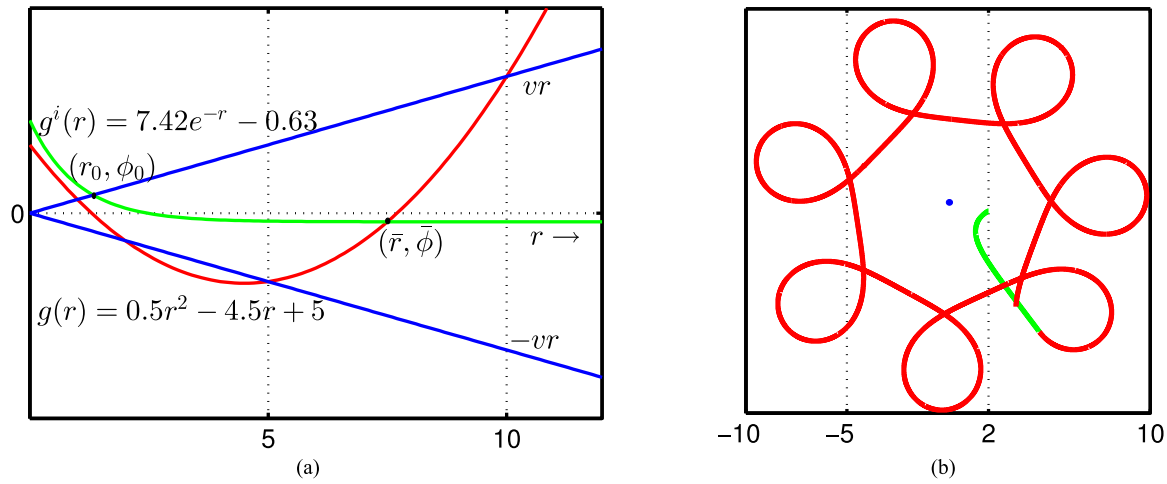

Fig. 6. Switching control strategy: green & red colours represent initial and desired patterns. (a) $g_K(r)s$. (b) Unicycle trajectory.

VI. Some Appealing Patterns & Their Generating Functions

The shape of a unicycle trajectory depends on the instantaneous (r, ϕ) values that is governed by $f(r)$. Hence, the unicycle can generate an array of heterogenous patterns by just varying $f(r)$. Any specified bounds of the trajectory in terms of r can be ensured by following Theorem 2.

In this section, we discuss the conditions on $f(r)$ in order to generate some mathematically appealing curves like hypotrochoids, epitrochoids, and spirals. Let $f(r) \in C^1$ and $f'(r) = df(r)/dr$. When the patterns are annular in $[R_{\min}, R_{\max}]$, the properties of $f(r)$ for $r \in [R_{\min}, R_{\max}]$ are given as follows:

1) $f(r)f'(r) > 0$: In this case, $f(r)$ does not change sign, so there are two possibilities: $f(r) > 0$ and $f'(r) > 0$ or $f(r) < 0$ and $f'(r) < 0$. For the former, $f(r)$ increases with increasing r, hence the unicycle always rotates in anticlockwise direction and the curvature given by $\kappa = |\frac{f(r)}{v}|$ is maximum at $R_{\max}$ and minimum at $R_{\min}$. In the latter case, the curvature behavior is similar. However, the unicycle rotates clockwise.The patterns generated by such $f(r)$ s are curves that look similar to hypotrochoids, as shown in Fig. 7(a).
2) $f(r)f'(r) < 0$: This is possible in two ways: $f(r) < 0$ and $f'(r) > 0$ or $f(r) > 0$ and $f'(r) < 0$. For the former case $f(r) < 0$ and the unicycle rotates clockwise. Hence, the curvature κ is maximum at $R_{\min}$ and minimum at $R_{\max}$. The patterns that satisfy this are similar to epitrochoids, as shown in Fig. 7(b). In the latter, we get the same patterns except that the unicycle can only rotate anticlockwise.
3) $f(r)$ *monotonic and* $f'(r)$ *changes sign*: In this case, the magnitude of κ is highest at the extrema with the sign of $f(r)$ being different. So the unicycle rotates both clockwise and anticlockwise, as shown in Fig. 7(x).
4) $f(r)$ *such that* $g_K(r) > 0$ *or* $g_K(r) < 0$ *for all* $r > 0$ *and* $S_K(f)$ *of* I_3 *form*: From (6), $g_K(r) > 0$ or $g_K(r) < 0$ for all $r(t) \geq 0$ ensures $\sin\phi(t)$ does not change sign for all time $t \geq 0$. Then, using (1), the line-of-sight angle, denoted by $\theta(t)$, is monotonic (as $\dot{\theta} = -v\sin\phi/r$ does not alter sign). $S_K(f)$ of I_3 form generates a trajectory where $r(t)$ is monotonic while varying from $\min(r(t))$ to ∞ resulting in spiral-like patterns as shown in Fig. 1(b).

Along with these aesthetically appealing curves, the control law can be designed to generate a wide variety of patterns depending on the imagination and choice of the user. Fig. 7 presents a plethora of patterns generated using continuous functions of range as given in Table I as input to the unicycle.

We observe in Fig. 7 that in some cases the unicycle covers the annulus densely [see Fig. 7(a)], whereas in others coarsely [Fig. 7(x)]. This behavior can be characterized by a variable θ defined as $\theta = \alpha - \phi$. The variable θ represents the line-of-sight angle between the unicycle and the target. From the proof of Theorem 1, we know that r and ϕ are periodic with the same period. So we can measure the change in θ for one period of r or ϕ. If change in θ is large, then the coverage of the annulus progresses faster as compared to when the change in θ is smaller. So, the change in θ as r varies from $R_{\min}$ to $R_{\max}$ can be a measure of the speed of the coverage.

We define a parameter *shift* represented by ν as

$$\nu = \overline{\theta} - \underline{\theta} \tag{15}$$

where $\overline{\theta}$ and $\underline{\theta}$ are the values of θ at two consecutive extremas of r, $R_{\max}$, and $R_{\min}$, respectively. From (3) and (6), $\frac{d\theta}{dr} = -\frac{g(r)}{r\sqrt{v^2r^2 - g^2(r)}}$. Then

$$\nu = -\int_{R_{\min}}^{R_{\max}} \frac{g(r)}{r\sqrt{v^2r^2 - g^2(r)}} dr. \tag{16}$$

$g(r)$ governs how fast the unicycle moves around the target. With a suitable choice of $g(r)$, we can also generate a closed curve which would require 2π to be divisible by ν.

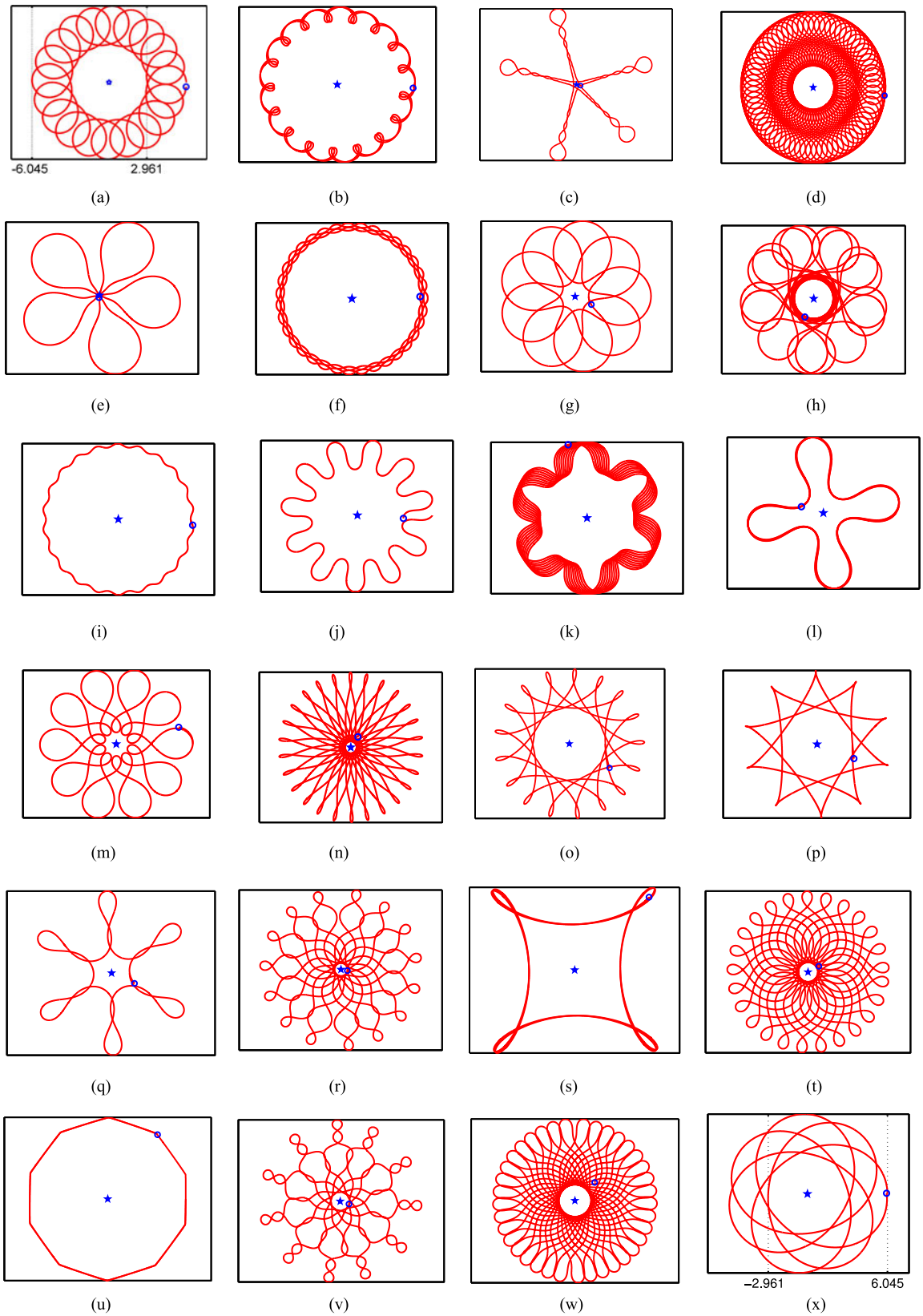

Fig. 7. Different types of patterns.

TABLE I
CONTROL INPUTS

	r_0	ϕ_0	v	$f(r)$		r_0	ϕ_0	v	$f(r)$
(a)	6.045	270	3/7	0.5 − 1/r	(m)	9.5353	270	1	1 − 4.5/r
(b)	2	90	1	$\tan(r)$	(n)	0.25	90	1	$0.5\cos(r)/\tan(2r)$
(c)	0.5	55	0.01	$0.01\cos\frac{100r}{1+r^2}$	(o)	0.25	90	1	$\cos(r)/\cos(3r)$
(d)	2	90	1	$0.5(\sin(0.1r^2)+2\cos(0.1r^2))$	(p)	0.25	90	1	$\sin(r)/\cos(3r)$
(e)	2	90	1	$0.01\cos\frac{1050r}{1+r^2}$	(q)	0.25	90	1	$0.25\cos(2r)/(\exp(-3r)\sin(0.5r))$
(f)	9.5353	270	1	$0.5\sin(10r)/\cos(r)$	(r)	0.25	90	1	$0.25\cos(3r)/(\exp(-r)\sin(0.5r))$
(g)	2	90	1	$0.5\sin\frac{10r^2}{1+r^2}$	(s)	0.25	90	1	$\cos(r)/(\exp(-r)\sin(5r))$
(h)	2	90	1	$0.5\sin\frac{10r^2}{1+r^3}$	(t)	0.25	90	1	$\cos(r)/(\exp(-r)\cos(0.5r))$
(i)	2	90	1	$\cot r$	(u)	0.25	90	1	$0.05\tan(\cos(10r)+\sin(15r))$
(j)	40	55	1	$\frac{\tan(0.1r)\log(0.01r)}{1+0.1r}$	(v)	0.5	90	1	$0.001r^2\cos(r)+r\sin(4r)$
(k)	40	55	1	$\frac{\cos(0.1r)\log(0.01r)}{1+0.1r}$	(w)	0.5	90	1	$0.1r^4\cos(r)+r\sin(4r)$
(l)	40	55	1	$0.2\sin(\log(r))$	(x)	6.045	270	3/7	$0.02r$

VII. CONCLUSION

The paper characterizes the trajectories of a system with unicycle kinematics when it is subject to control laws that are continuous functions of range. The advantage of these control laws is that by the use of only range information, the unicycle can generate a variety of aesthetically appealing patterns. The use of minimal information also results in reduced operational cost. Mathematical analysis shows that the use of range information results in two categories of patterns: annular with radial distance varying periodically between its maximum and minimum or unbounded where radial distance monotonically increases from the minimum value. We propose a design strategy for control laws so that the unicycle generates any desired annular pattern. We also prove that the agent can trace any arbitrary annular pattern while starting from any initial position of the agent by using a simple switching of control laws. It is found that most of the annular patterns are not closed, which means that every point on the annulus is visited. This makes these patterns suitable to serve coverage applications. As future work, the range of patterns can be extended by incorporating other measurement parameters in the input, varying the speed of the agent, and moving the target point A feedback controller can also be designed to further ensure stability and robustness.

REFERENCES

[1] M. Pavone and E. Frazzoli, "Decentralized policies for geometric pattern formation and path coverage," *J. Dyn. Syst. Meas. Control*, vol. 129, no. 5, pp. 633–643, 2007.

[2] M. Mischiati and P. S. Krishnaprasad, "The dynamics of mutual motion camouflage," *Syst. Control Lett.*, vol. 61, pp. 894–903, 2012.

[3] K.-K. Oh, M.-C. Park, and H.-S. Ahn, "A survey of multi-agent formation control," Automatica, vol. 53, no. 3, pp. 424–440, 2015.

[4] I. Suzuki and M. Yamashita, "Distributed anonymous mobile robots: Formation of geometric patterns," *SIAM J. Comput.*, vol. 28, no. 4, pp. 1347–1363, 1999.

[5] K. Sugihara and I. Suzuki, "Distributed motion coordination of multiple mobile robots," in *Proc. 5th IEEE Int. Symp. Intell. Control*, 1990, pp. 138–143.

[6] J. A. Marshall, M. E. Broucke, and B. A. Francis, "Pursuit formations of unicycles," *Automatica*, vol. 42, no. 1, pp. 3–12, 2006.

[7] J. A. Marshall, M. E. Broucke, and B. A. Francis, "Formations of vehicles in cyclic pursuit," *IEEE Trans. Autom. Control*, vol. 49, no. 11, pp. 1963–1974, Nov. 2004.

[8] P. Lin and Y. Jia, "Distributed rotating formation control of multi-agent systems," *Syst. Control Lett.*, vol. 59, no. 10, pp. 587–595, 2010.

[9] E. W. Justh and P. S. Krishnaprasad, "Equilibria and steering laws for planar formations," *Syst. Control Lett.*, vol. 52, no. 10, pp. 25–38, 2004.

[10] M. I. El-Hawwary, "Three-dimensional circular formations via set stabilization," *Automatica*, vol. 54, no. 4, pp. 374–381, 2015.

[11] K. S. Galloway, E. W. Justh, and P. S. Krishnaprasad, "Portraits of cyclic pursuit," in *Proc. 42nd IEEE Conf. Decis. Control*, Orlando, FL, USA, Dec. 2011, pp. 2724–2731.

[12] K. S. Galloway, E. W. Justh, and P. S. Krishnaprasad, "Symmetry and reduction in collectives: Low dimensional cyclic pursuit," *Proc. Roy. Soc. A*, 2016. [Online]. Available: https://doi.org/10.1098/rspa.2016.0465.

[13] J. A. Marshall and D. Tsai, "Periodic formations of multivehicle systems," *IET Control Theory Appl.*, vol. 5, no. 2, pp. 389–396, 2011.

[14] J.-C. Juang, "On the formation patterns under generalized cyclic pursuit," *IEEE Trans. Autom. Control*, vol. 58, no. 9, pp. 2401–2405, Sep. 2013.

[15] P. Tsiotras and L. I. R. Castro, "Extended multi-agent consensus protocols for the generation of geometric patterns in the plane," in *Proc. Amer. Control Conf.*, San Francisco, CA, USA, Jun. 2011, pp. 3850–3855.

[16] P. Tsiotras and L. I. Reyes Castro, "The artistic geometry of consensus protocols," in *Controls and Art*. New York, NY, USA: Springer-Verlag, 2014, pp. 129–153.

[17] A. Morro, A. Sgorbissa, and R. Zaccaria, "Path following for unicycle robots with an arbitrary path curvature," *IEEE Trans. Robot.*, vol. 27, no. 5, pp. 1016–1023, Oct. 2011.

[18] A. Doosthoseini and C. Nielsen, "Coordinated path following for a multi-agent system of unicycles," in *Proc. 42nd IEEE Conf. Decis. Control*, Fleorence, Italy, Dec. 2013, pp. 2894–2899.

[19] X. Xiang, L. Lapierre, C. Liu, and B. Jouvencel, "Path tracking: Combined path following and trajectory tracking for autonomous underwater vehicles," in *Proc. Int. Conf. Intell. Robots Syst.*, San Francisco, CA, USA, Sep. 2011, pp. 3558–3563.

[20] T. Tripathy and A. Sinha, "Guidance of an autonomous agent for coverage applications using range only measurement," in *Proc. AIAA Guid. Navig. Control Conf.*, Boston, MA, USA, Aug. 2013. [Online]. Available: http:dx.doi.org/10.2514/6.2013-5095

[21] T. Tripathy and A. Sinha, "A guidance law for a mobile robot for coverage applications: A limited information approach," in *Proc. 3rd Int. Conf. Adv. Control Optim. Dyn. Syst.*, Kanpur, India, Mar. 2014, pp. 437–442.

[22] T. Tripathy and A. Sinha, "A control scheme to achieve coverage using unicycles," in *Proc. Indian Control Conf.*, Chennai, India, Jan. 2015, pp. 494–499.

[23] T. Tripathy and A. Sinha, "Generating patterns with a unicycle," *IEEE Trans. Autom. Control*, vol. 61, no. 10, pp. 3140–3145, Oct. 2016, doi: https://doi.org/10.1109/TAC.2015.2503891.
[24] G. F. Simmons, *Differential Equations With Applications and Historical Notes*, 2nd ed. New York, NY, USA: McGraw-Hill, 2003.

Twinkle Tripathy (S'14) received the B.Tech. degree in electronics and instrumentation engineering from the College of Engineering and Technology, Bhubaneswar, India, in 2011.

She is currently a research scholar with the Systems and Control Engineering, Indian Institute of Technology Bombay, Mumbai, India. Her current research interests include guidance and control of autonomous agents, cooperative control, and missile guidance.

Arpita Sinha (M'09) received the Ph.D. degree in aerospace engineering from Indian Institute of Science, Bangaluru, India, in 2007.

Since 2009, she has been with the Systems and Control Engineering, Indian Institute of Technology (IIT) Bombay, Mumbai, India. Prior to joining IIT Bombay, she was a Postdoctoral Researcher at Cranfield University, Shrivenham, U.K. Her research interests include the guidance and control of multiple autonomous vehicles, path planning, consensus algorithms, and distributed decisions making systems.